

A coupled solver approach for multiphase flow problems

Berend G.M. van Wachem, Aldo Benavides, and Vinay R. Gopala

Department of Applied Mechanics, Chalmers University of Technology

SE-41296 Gothenburg

E-mail: berend@chalmers.se

Keywords: numerical multiphase flow, coupled solving, VOF, Eulerian

Abstract

Because of increasing computer speed and memory, the numerical solution of the incompressible Navier-Stokes equations by a fully coupled approach is an attractive and emerging trend in computational fluid dynamics (CFD) calculations. The main advantage of this approach is an increased robustness due to the implicit treatment of the pressure velocity coupling Schneider and Raw (1987); Deng et al. (2001).

Although the equations describing multiphase flows appear similar to single-phase flow equations, their nature is often much more difficult due to the presence of volume fractions, large source terms, and gradients of these as well as density. This makes the requirement for a robust solving approach even more desirable.

Almost all multiphase CFD solvers today are based upon standard decoupled approaches (*e.g.* SIMPLE, SIMPLER, PISO, fractional step, and other pressure projection methods Ferziger and Peric (2002)) and most often employ a staggered variable arrangement. In this paper, momentum weighted interpolation is used to determine analytical expressions for the cell face velocities which are employed in the multiphase continuity equation in a collocated variable arrangement. A special approach is adopted for the momentum weighted interpolation to handle large source terms, volume fractions, and gradients of these. The resulting linearized equations are solved in a fully coupled manner.

The fully coupled method is validated with the lid driven cavity data of Ghia et al. (1982), and demonstrated on two practical multiphase cases. Firstly, the method is demonstrated simulating volume of fluid (VOF) computations of a gas-liquid flow case. Secondly, the method is demonstrated on solving the continuous part of an Euler-Lagrange gas-solid flow problem. The difficulties in the first case are large source terms and gradients of density, and in the second case the presence of volume fraction and gradients hereof, as well as source terms.

The results are in accordance with results from the staggered segregated approach. Moreover, due to the collocated variable arrangement, complex geometries can be easily handled. Both robustness and computational efficiency of this fully coupled approach are shown.

Introduction

There is no dispute that on Cartesian grids, computation of incompressible flow is best performed with the staggered scheme proposed by Harlow and Welch (1965). However when the grid is arbitrary, the use of collocated schemes is prevalent and more natural. One of the reasons for this, is that the generalization from Cartesian to a general case grid is quite straightforward. Staggered grids are much more complicated and often suffer from accuracy problems on non-uniform grids due to the use of Christoffel symbols Aris (1962) which are difficult to compute accurately on general grids Wesseling et al. (1998). Although some researchers have proposed remedies to this, *e.g.* Perot (2000); Wenneker et al. (2003), the approach is still less natural than employing a collocated discretisation.

However, there are a number of drawbacks when employing collocated grids as well. A straightforward discretisation on

a collocated grid results in pressure oscillations. To remedy this, the discretisation for the momentum convective velocity needs to differ from the continuity convection. Currently, there are two main approaches: the pressure-weighted interpolation Rhie and Chow (1983); Zwart (1999) and the physical consistent interpolation Schneider and Raw (1987); Deng et al. (1994). Moreover, applying source terms and body forces in the equation also introduces problems, as they cannot be precisely matched by the discretisation of the pressure gradient stencil.

In the physical consistent interpolation, first proposed by Schneider and Raw (1987), the complete momentum equation is averaged to the cell faces. The resulting expression at the cell faces is then used to close the continuity equation. Although the method is very elegant, the major problem of the method is the interpolation of the viscous terms. Due to the size of the discretisation stencil of the viscous terms, their interpolated stencil becomes rather

large Deng et al. (1994) and may not perform well in near-wall regions. Moreover, the method is rather complex to code for a multiphase case, where care has to be taken with volume fractions and various kinds of source terms.

In pressure-weighted interpolation Rhie and Chow (1983); Zwart (1999), the face velocity for the convective term in the continuity equation is determined by subtracting the difference between the pressure gradient and the interpolated pressure gradient from the linearly determined face velocity. Mathematically, this can be seen as a filter for the velocity and pressure, forcing the local pressure profile to be linear, without affecting the accuracy of the continuity equation. The drawback of this approach becomes clear in the presence of source terms and gradients of density and volume fraction, as the physical pressure profile is no longer locally linear. This is one of the subjects of the current article.

Another benefit of collocated grids is that its discretisation enables to fully couple the velocity and pressure equations, as will be shown in this article. Although coupling the velocity and pressure equations lead to an increase in memory usage, the large advantage is increased robustness due to the implicit and global treatment of the pressure-velocity coupling. Moreover, fully coupled methods are reported to have an overall favourable computational cost when a suitable preconditioner and solver are employed Ammara and Masson (2004).

This article treats the derivation of a three dimensional fully coupled transient solver for viscous multiphase flows in the presence of large source terms and large gradients in density and volume-fraction. The abilities of the framework are shown on two practical multiphase cases, *i.e.* a volume of fluid (VOF) simulation of a droplet including surface tension, and an Euler-Lagrange simulation containing air mixed with spherical particles.

Numerical method

In incompressible flow calculations, straightforward discretisation of the Navier-Stokes equations leads to an ill-conditioned discretised problem as the diagonal for the continuity equation contains zeros, since pressure does not appear. There are a number of ways in dealing with this problem. Firstly, the most employed approach is to use segregated or projection methods Patankar (1980); Ferziger and Peric (2002). In these frameworks, the momentum equations are solved with a guessed pressure, and thereafter the pressure is corrected, so the velocity field satisfies the continuity equation. This procedure is repeated until the velocity field nearly satisfies the momentum equation as well.

Secondly, the system can be solved coupled. This can be done with a penalty formulation Vanka (1985), or using a density based framework and, for instance, applying artificial compressibility Wesseling (2000). In the current paper, we employ an incompressible approach, in which the face velocities required for discretising the continuity equation

are interpolated from the discretised momentum equations at cell centers Rhie and Chow (1983); Schneider and Raw (1987); Deng et al. (2001). The extension to compressible flows is straightforward.

Single Phase Flow

For illustration, the method is explained for the single phase incompressible flow equations, and the extension to multiphase flow equations will be treated in the next section. Consider the single phase flow continuity equation,

$$\frac{\partial}{\partial x^i} u^i = 0 \quad (1)$$

or in its first discretised form,

$$\sum_{f=\text{faces}} M_f = \sum_{f=\text{faces}} u_f^i s_f^i = 0 \quad (2)$$

Hence, an expression for the face velocity, u_f^i needs to be obtained. This will be done from manipulating the momentum equations. The momentum equations of an incompressible single phase flow including source terms are

$$\rho \frac{\partial u^j}{\partial t} + \rho \frac{\partial}{\partial x^i} (u^i u^j) = - \frac{\partial p}{\partial x^j} + \frac{\partial \tau_{ij}}{\partial x^i} - R u^j - S^j \quad (3)$$

where the first term indicates the transient contribution and the second the convective contribution. The source terms are given by S^j , which is a general source term (not linear in velocity) and a linearized source term, R , representing the part of the source term which is linear in velocity. The cell centered finite volume discretisation at P of the velocity terms for one direction of the equation 3, is of the form

$$\left[\frac{\rho V_P}{\Delta t} + a_P^{(u^j)} + V_P R_P^{(u^j)} \right] u_P^j = \left[\sum_{nb} a_{nb}^{(u^j)} u_{nb}^j \right]_P - V_P \left[\sum_{nb} b_{nb}^{(j)} P_{nb} + S^{u^j} \right] + \left[\frac{\rho V_P}{\Delta t} \right]_P u_P^{j,O} \quad (4)$$

where a and b are coefficients obtained from the discretisation stencils, and V_P is the volume of the computational cell surrounding point P . The net force driving the flow is given by $\left[\frac{\partial p}{\partial x^j} + S^{u^j} \right]$, and is defined as

$$\widetilde{\frac{\partial p}{\partial x^j}} = \left[\frac{\partial p}{\partial x^j} + S^{u^j} \right] \quad (5)$$

It is important to treat the pressure gradient and the sources similar, as their sum is the contribution to accelerating the fluid. With this, Equation 4 becomes

$$\left[1 + \frac{\rho}{\Delta t} \frac{V_P}{a_P^{(u^j)} + V_P R_P^{(u^j)}} \right] u_P^j = \left\{ \frac{\left[\sum_{nb} a_{nb}^{(u^j)} u_{nb}^j \right]_P}{a_P^{(u^j)} + V_P R_P^{(u^j)}} \right\} - V_P \frac{\left[\frac{\partial p}{\partial x^j} \right]_P}{a_P^{(u^j)} + V_P R_P^{(u^j)}} + \left[\frac{\rho}{\Delta t} \right]_P \frac{V_P}{a_P^{(u^j)} + V_P R_P^{(u^j)}} u_P^{j,O} \quad (6)$$

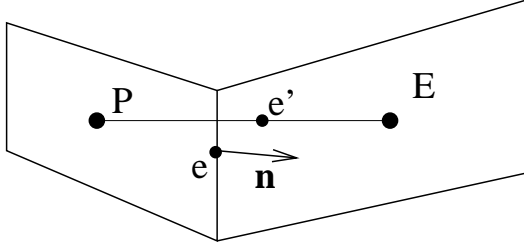


Figure 1: A two-dimensional boundary fitted cell (P) with its east neighbour (E). Halfway the line connecting points P and E is point e' . The center of the face between P and E is shown by point e , and the local normal at this point is given by n^i .

or, with the abbreviations,

$$c = \frac{\rho}{\Delta t} \quad (7)$$

$$d^{(u^j)} = \frac{V_P}{a_P^{(u^j)} + V_P R_P^{(u^j)}} \quad (8)$$

$$\widetilde{u}^j = \left\{ \frac{\left[\sum_{nb} a_{nb}^{(u^j)} u_{nb}^j \right]_P}{a_P^{(u^j)} + V_P R_P^{(u^j)}} \right\} \quad (9)$$

For cell P equation 6 becomes

$$\left[1 + c_P d_P^{(u^j)} \right] u_P^j = \widetilde{u}^j_P - d_P^{(u^j)} \left[\frac{\partial p}{\partial x^j} \right]_P + c_P d_P^{(u^j)} u_P^{j,O} \quad (10)$$

A similar equation can be written for all cell centers, taking boundary conditions into account. Figure 1 shows two cell center nodes (P and E) with a line connecting these two points. The point e' is defined in such a way that it lies in the center of this line connecting the nodes P and E . An analogous equation can be written down for the velocity at point e' ,

$$\left[1 + c_{e'} d_{e'}^{(u^j)} \right] u_{e'}^j = \widetilde{u}^j_{e'} - d_{e'}^{(u^j)} \left[\frac{\partial p}{\partial x^j} \right]_{e'} + c_{e'} d_{e'}^{(u^j)} u_{e'}^{j,O} \quad (11)$$

and an expression for the velocity at point e' is obtained by using the velocity expressions for points E and P . This equation can be directly used to close the discretised continuity equation. Now, the continuity equation is dependent upon the pressure field, and a coupled formulation can be given as,

$$\begin{pmatrix} \dots & \dots & \dots & \dots \\ \dots & \dots & \dots & \dots \\ \dots & \dots & \dots & \dots \\ \dots & \dots & \dots & \dots \end{pmatrix} \begin{pmatrix} u_1 \\ u_2 \\ u_3 \\ p \end{pmatrix} = \begin{pmatrix} RH_{u_1} \\ RH_{u_2} \\ RH_{u_3} \\ RH_p \end{pmatrix} \quad (12)$$

where the diagonals are non-zero. A problem consisting of $n_1 n_2 n_3$ computational cells, leads to a matrix size of $4n_1 n_2 n_3 \times 4n_1 n_2 n_3$.

Eulerian-Eulerian discretisation

The discretized momentum equation for phase k in direction j can be written as

$$\left[\frac{\rho_k V_P}{\Delta t} \alpha_{k,P} + a_P^{(U_k^j)} + V_P R_{k,P} \right] U_{k,P}^j = \left[\sum_{nb} a_{nb}^{(U_k^j)} U_{k,nb}^j \right]_P - V_P \left[\alpha_k \frac{\partial P}{\partial x^j} - S_k^j - \alpha_k T_k^j \right]_P + \left[\frac{\rho_k V_P}{\Delta t} \right]_P \alpha_{k,P}^o U_{k,P}^{j,o} \quad (13)$$

From Equation 13 the net force on phase k is given by

$$\left[\frac{\partial P}{\partial x^j} \right]_k = \alpha_k \frac{\partial P}{\partial x^j} - \alpha_k \Lambda^j - \alpha_k T_k^j \quad (14)$$

where $\Lambda^j = S_k^j / \alpha_k$. After division with $\left(a_P^{(U_k^j)} + V_P R_{k,P} \right)$ Equation 13 becomes

$$\left[1 + \frac{\rho_k}{\Delta t} \frac{\alpha_{k,P} V_P}{a_P^{(U_k^j)} + V_P R_{k,P}} \right] U_{k,P}^j = \left\{ \frac{\left[\sum_{nb} a_{nb}^{(U_k^j)} U_{k,nb}^j \right]_P}{a_P^{(U_k^j)} + V_P R_{k,P}} \right\} - V_P \frac{\left[\frac{\partial P}{\partial x^j} \right]_{k,P}}{a_P^{(U_k^j)} + V_P R_{k,P}} + \frac{\rho_k}{\Delta t} \frac{V_P}{a_P^{(U_k^j)} + V_P R_{k,P}} \alpha_{k,P}^o U_{k,P}^{j,o} \quad (15)$$

Now, we define the variables c_k , $d^{(U_k^j)}$, and $\widetilde{U}_{k,P}^j$ as follows

$$c_k = \frac{\rho_k}{\Delta t} \quad (16)$$

$$d_P^{(U_k^j)} = \frac{V_P}{a_P^{(U_k^j)} + V_P R_{k,P}} \quad (17)$$

$$\widetilde{U}_{k,P}^j = \left\{ \frac{\left[\sum_{nb} a_{nb}^{(U_k^j)} U_{k,nb}^j \right]_P}{a_P^{(U_k^j)} + V_P R_{k,P}} \right\} \quad (18)$$

With these abbreviations, Equation 15 becomes for cell P

$$\left[1 + c_k \alpha_{k,P} d_P^{(U_k^j)} \right] U_{k,P}^j = \widetilde{U}_{k,P}^j - d_P^{(U_k^j)} \left[\frac{\partial P}{\partial x^j} \right]_{k,P} + c_k d_P^{(U_k^j)} \alpha_{k,P}^o U_{k,P}^{j,O} \quad (19)$$

The values of the velocities are required at cell faces (see Figure 1). An analogous equation is written down for the point in the center of the line PE , e' .

$$\left[1 + c_k \alpha_{k,e'} d_{e'}^{(U_k^j)} \right] U_{k,e'}^j = \widetilde{U}_{k,e'}^j - d_{e'}^{(U_k^j)} \left[\frac{\partial P}{\partial x^j} \right]_{k,e'} + c_k d_{e'}^{(U_k^j)} \alpha_{k,e'}^o U_{k,e'}^{j,O} \quad (20)$$

Now, we use equations 19 to close the sum of the continuity equations and obtain a coupled system for the velocity field, the pressure field, and the volume fractions.

Treatment of source terms

One of the most important features of multiphase flows equations, is the presence of source terms originating from closure models. These source terms are relatively large and have large gradients over the domain, due to the presence of interfaces (gas-liquid), drag forces (droplets, particles), and a varying gravity force due to density changes in the domain.

Although constant body forces, such as gravity for a constant density flow, can be fairly easily dealt with Choi et al. (2003), this is generally not the case when the sources are varying, as in most multiphase flows. In these cases, it is important that the discretisation of the pressure gradient matches the representation of the local source terms. When the source terms are a function of a gradient, for instance the surface tension force, this is fairly natural, as the discretised gradient operator for the source terms should match the discretised gradient operator for the pressure. However, in a general case, the source terms should closely match the discretisation of the gradient operator applied for pressure. This operator should be applied on an integral form of the local source term,

$$Q \approx \int_V S^i dx^i \quad (21)$$

$$(22)$$

so that

$$\widetilde{S}^i \approx \frac{\partial Q}{\partial x^i} \quad (23)$$

Although the formulation of Q is probably not unique, we have chosen to base Q upon the co-variant cell face vectors, employing weighting factors of $\frac{1}{2}$ to determine the cell face source terms. With Q defined at the cell face center, an approximation of the gradient of Q can be made at the cell center,

$$\widetilde{S}^i_P = \frac{1}{\Delta\Omega} \sum_{f=\text{faces}} Q_f s_f^i \quad (24)$$

which is similar to the discretisation of the pressure gradient. This representation is employed in the discretised cell face velocity equation. Note that in some cases, the actual direction of the source terms is important, as in gravity, and the direction should be maintained in the procedure outlined above.

Boundary conditions

Special care needs to be taken regarding boundary conditions for the pressure. The pressure variable appears in two places, in the continuity equation and in the momentum equations. At boundaries where the velocity is specified (Dirichlet), no additional pressure terms are required in the cell face velocity interpolation. The remaining pressure terms, in the momentum equations, can be determined by extrapolation.

At boundaries where the pressure is directly specified, velocity is typically extrapolated. In this case, the boundary pressure can be directly specified in both the continuity

equation as well as the momentum equation. An excellent discussion of the boundary conditions can be found in Zwart (1999).

Solving strategy

The coefficients in the discretized equations are determined from the discretisation stencils from the individual terms. The convective terms are discretized using a higher order upwind scheme, the stress and pressure terms are discretized centrally (applying Gauss law), and the transient term is discretized with a second order backward scheme (trapezium rule).

The resulting system to be solved, Equation 12, results in a block-banded linear matrix with slightly less favourable coefficients than the systems in the segregated counterpart. For instance, if the whole pressure term discretisation is taken implicit, the resulting one dimensional coefficients for the continuity equation are $(\frac{1}{4} \quad -1 \quad \frac{3}{2} \quad -1 \quad \frac{1}{4})$ which is less favourable than the regular poisson stencil. Although applying deferred correction improves the convergence, it does require additional outer iterations to be taken and leads to a loss in robustness. The main numerical bottleneck consists in limiting the effort devoted to the formation of a reliable preconditioner.

The parallel code developed is based upon the numerical libraries of PETSc (Portable Extensible Toolkit for Scientific computing) Balay et al. (2006, 2004, 1997) which provide a large suite of parallel linear and non-linear equation solvers. In this work, a block-ILU preconditioner is employed with the BiCGSTAB Krylov subspace solver Bruaset (1995).

Validation

To validate the procedure and its implementation, a lid-driven square cavity flow is considered, which is extensively used as a benchmark for CFD code validation. This case was previously studied by Ghia et al. (1982), whom provide a highly accurate solution. The problem consist in a square box with three fixed walls, the fluid flow is generated by the movement of the upper wall.

In the current work, simulations at two different Reynolds numbers are performed. The simulations are carried out in two uniform Cartesian meshes with 70×70 and 140×140 grid points for Reynolds numbers 100 and 400, respectively. Figures 2(a) and 2(b) show a comparison of the velocity distributions at horizontal ($y = 0.5$) and vertical ($x = 0.5$) centerlines of the cavity at Reynolds numbers $Re = 100$ and $Re = 400$, respectively. The results computed using the procedure outlined in this work agree very well with the data from Ghia et al. (1982). The coarse mesh results shows a peak deviation of 10% in the velocity profiles at Reynolds number $Re = 400$. The cavity flow is characterized by a main vortex in the centre and two secondary vortices at the lower corners for cases with Reynolds number less than

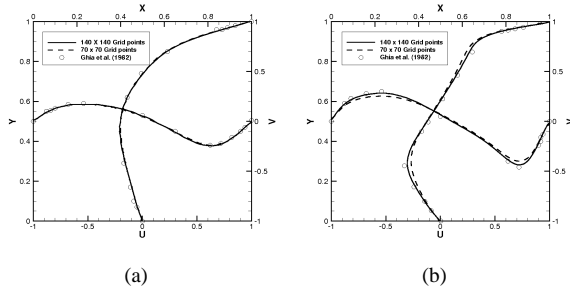


Figure 2: Velocity profiles at centerline of the cavity. (a) $Re = 100$; (b) $Re = 400$.

1000. Figure 3 shows the streamline contours for Reynolds 100 and 400, the characteristic flow behavior can be easily observed in both simulations. The secondary vortices increase the size with the increase of the Reynolds number.

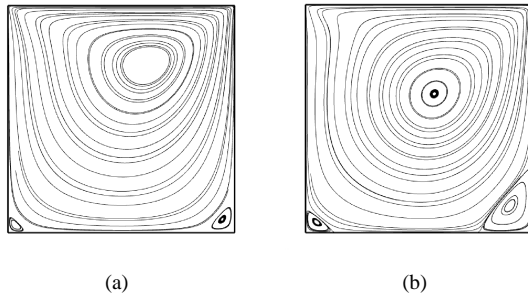


Figure 3: Lid-drive cavity flow, streamline contours. (a) $Re = 100$; (b) $Re = 400$.

Multiphase Flow systems

In the present work, we study two types of multiphase flow systems. The first type is the Volume of Fluid (VOF), and the second type is the modeling of the interstitial fluid, the Eulerian phase, in a Lagrangian particle simulation. Both cases have varying source terms (surface tension force and gravity force) as well as gradients in density or volume fraction. The difficulties in modelling these are discussed below.

Volume of Fluid method

The VOF method is a powerful tool for modeling incompressible fluid flows which contain a free surface e.g. Hirt and Nicholls (1981). In the VOF method, the fluid location is recorded by employing a volume-of-fluid function, or color function, which is defined as unity within the fluid regions and zero elsewhere. In practical numerical simulations employing a VOF algorithm, this function is unity in computational cells occupied completely by fluid of phase 1, zero in regions occupied completely by phase 2, and a value between these limits in cells which contain a free surface. In the VOF algorithm, the color function is semi-discontinuous while in the closely related level-set algorithm, this function is completely continuous. The set of equations which are

required to solve for this method are

$$\frac{\partial}{\partial x^i} u^i = 0 \quad (25)$$

$$\rho \frac{\partial u^j}{\partial t} + \rho \frac{\partial}{\partial x^i} (u^i u^j) = -\frac{\partial}{\partial x^j} p + \frac{\partial}{\partial x^i} \tau_{ij} - S^j \quad (26)$$

$$\frac{\partial \xi}{\partial t} + \frac{\partial u^i \xi}{\partial x^i} = 0 \quad (27)$$

where ρ is the density of the local fluid, p the local pressure, S the surface tension, τ the viscous stress tensor, ξ is the color-function, and u the velocity field of the local phase. The surface tension in the framework of the VOF method is usually applied in the form of the continuum framework Brackbill et al. (1992),

$$S^j = \sigma \kappa(\mathbf{x}) n^j(\mathbf{x}) \Gamma(\mathbf{x}) \quad (28)$$

where σ is the surface tension and is assumed constant, Γ is an interface indicator function, and κ is the curvature of the interface. In the most popular continuum surface tension model, by Brackbill et al. (1992), the interface indicator, the curvature of the interface, and the interface normal are directly related to the color function,

$$\Gamma(\mathbf{x}) = |\nabla \xi(\mathbf{x})| \quad (29)$$

$$\kappa(\mathbf{x}) = -\nabla \cdot \mathbf{n}(\mathbf{x}) \quad (30)$$

where \mathbf{n} is defined as the normal at the gas-liquid interface. Solving the advection equation 27 for the color function using regular advection techniques tend to rapidly smear the interface over three or four mesh cells. Many algorithms have been designed to solve equation 27 such that a sharp interface is retained. In the present work flux-corrected transport (FCT) algorithm is used to track the interface.

FCT is based on the idea that a suitable combination of up and downwind fluxes can be formulated that eliminates both the diffusiveness of the upwind scheme and the instability of the downwind scheme. The idea of adjusting fluxes calculated with a higher order (non-monotonic) advection scheme to improve the monotonicity of the final result was introduced by Boris and Book (1973) and was generalized and extended to multidimensions by Zalesak (1979). The method involves several stages of calculation. First, an intermediate value of $\xi(\xi^*)$ is determined using a lower order monotonic (and hence diffusive) advection scheme. The scheme for solving the one-dimensional version of equation 27 (for mesh cell i) is symbolically written as

$$\xi_i^* = \xi_i^n - \frac{1}{\delta x} \left(F_{i+1/2}^L - F_{i-1/2}^L \right), \quad (31)$$

where F^L represents the lower order flux. Further an anti-diffusive flux (F^A) is defined that attempts to correct the numerical diffusion resulting from the lower order scheme. An estimate of the anti-diffusive fluxes is given by the difference between the higher and lower order flux approximations:

$$F_{i+1/2}^A = F_{i+1/2}^H - F_{i+1/2}^L. \quad (32)$$

Application of the entire anti-diffusive flux would simply result in the unstable higher order flux being used, thus correction factors q are introduced that limit the anti-diffusive

fluxes. The correction factors are calculated to ensure that no new extrema are introduced into the solution after application of the anti-diffusive fluxes. The minimum and maximum values allowed for a mesh cell i are based on ξ^n and ξ^* in cell i and its two neighbours, $i - 1$ and $i + 1$. Details of the procedure used to limit the fluxes are described in Zalesak (1979). The final step of flux-corrected transport algorithm is to apply the anti-diffusive fluxes with the correction factors and obtain the values of the color function at the new time:

$$\xi_i^{n+1} = \xi_i^* - \frac{(q_{i+1/2} F_{i+1/2}^A - q_{i-1/2} F_{i-1/2}^A)}{\delta x}. \quad (33)$$

The above FCT algorithm is extended to multi-dimensions by direction-split implementation. Rudman Rudman (1997) has shown that the direction split FCT gives superior results compared to multidimensional extension proposed by Zalesak (1979). Unfortunately, the method does not work well for flows with vorticity; the method becomes quite diffusive in such cases.

The additional numerical difficulties arise in the discontinuous property of the local density as well as the large source terms and source term gradients near the interface due to the surface tension and gravity. Typically, near the interface, the densities are harmonically averaged to obtain their cell face value to prevent over-representation of one of the phases. The source term due to the surface tension is treated by noticing that the interface normal contains the gradient of the colorfunction ξ , which can be split up in the same way as pressure when determining the values for face velocity. The terms in front of the interface normal are smoothed to avoid wiggles. The source term due to gravity is treated as outlined above, keeping in mind that the direction of gravity should remain constant, independent upon the formulation of the function Q .

Eulerian-Lagrangian fluid-particle method

Due to increasing computer power, discrete particle models, or Lagrangian models, have become a very useful and versatile tool to study the hydrodynamic behavior of particulate flows. Next to the continuous phase equations, the Newtonian equations of motion are solved for each individual particle, and a collision model is applied to handle particle encounters. In the numerical framework, we consider both the behaviour of the particles (which details are not treated in this article) as well as the behaviour of the interstitial fluid. The motion of the gas-phase is calculated from the volume averaged gas-phase governing equations as put forward by Jackson (1997), with the continuity equation

$$\frac{\partial \alpha \rho}{\partial t} + \frac{\partial}{\partial x^i} (\alpha \rho u^i) = 0 \quad (34)$$

where α represents the volume fraction of the fluid, ρ the intrinsic density of the fluid, and u^i the velocity field of the fluid. The volume fraction is given by the location and number of particles from the Lagrangian calculations. The mo-

mentum equations are given by

$$\frac{\partial \alpha \rho u^j}{\partial t} + \frac{\partial}{\partial x^i} (\alpha \rho u^j u^i) = \frac{\partial}{\partial x^i} \alpha \tau^{ij} - \alpha \frac{\partial}{\partial x^j} p + S u^j + T^j \quad (35)$$

where τ_a^{ij} represents the stress tensor of the fluid, p represents the pressure, and S and T represent the source terms due to interphase momentum transfer from the fluid phase to the particle phase.

The behaviour of the particles is resolved with a Lagrangian model van Wachem et al. (2001); Hoomans et al. (1996); Lees and Edwards (1972); Ladd and Walton (1989); Walton (1993) in which the particle interactions are dealt with a soft-sphere particle interaction model. Details of this approach can be found in the above references.

The additional numerical difficulties arise in the presence of the additional volume fraction α , as well as the large source terms and terms linear in velocity, and gradients of both, caused by the drag of the particles and gravity upon the gas phase. This is resolved with the source term projection method outlined above, where care should be taken that the direction of the gravity remains unaffected by the representation of Q . Compared to the single phase continuity equation, an additional term is added.

Results

Relatively simple cases were set-up to compare the outlined coupled approach to our earlier work employing a staggered segregated approach for the two types of multiphase flow.

VOF method

In the VOF method, the coupled approach was compared to the staggered segregated approach described in van Wachem and Schouten (2002). The approach from van Wachem and Schouten (2002) employed a novel piecewise linear Lagrangian framework to compute the evolution of the colorfunction, where in this work the FCT scheme is employed, which has a more diffusive nature and does not perform well in flows containing vorticity.

Two test-cases have been run with the coupled approach, both starting with a square block of water, $\rho = 1000 \text{ kgm}^{-3}$; $\nu = 1.0 \cdot 10^{-3} \text{ Nsm}^{-2}$, in a 10 cm wide column filled with air, $\rho = 1.28 \text{ kgm}^{-3}$; $\nu = 1.8 \cdot 10^{-5} \text{ Nsm}^{-2}$. In both cases, surface tension is applied to the interface, $\sigma = 0.070 \text{ Nm}^{-1}$. In the first case, no gravity is included. Figure 4 shows the values of the colorfunction, red denoting water and blue denoting air. The interface starts to approach a spherical form, in the process it overshoots that form and goes back and forth until the viscosity dampens the oscillations and a stationary spherical form is obtained. The results are very similar to the results obtained with the staggered segregated approach. The total computational cost is about 10 % lower compared to the segregated approach, which is not very much. This is due to the harmonic averaging of the density terms surrounding the interface, which makes the coefficient lay-out and magnitude

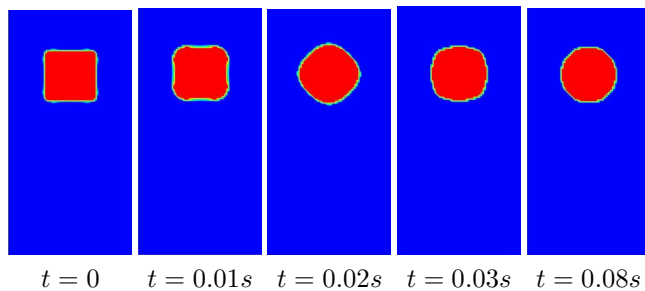


Figure 4: The values of the colorfunction, denoting water (red), or air (blue). A “square” body of water (left) in air without gravity transforming to a spherical shape due to surface tension. The column is 10 cm wide and 25 cm high and consists out of 64x192 computational cells.

difficult. The main numerical bottleneck consists in a reliable preconditioner and solver, and choosing a balance between coupled and deferred correction. At this time, we have not optimized this.

The second case is similar to the first case, but including gravity. Figure 5 shows the values of the colorfunction for this case, red denoting water and blue denoting air. Next to the droplet becoming more spherical due to the surface tension, it also moves downward and deforms due to the interaction with air. Although the results for small timevalues

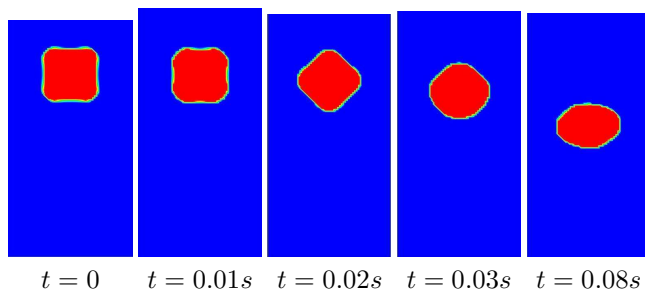


Figure 5: A “square” body of water (left) in air transforming and moving downward due to gravity. The column is 10 cm wide and 25 cm high and consists out of 64x192 computational cells.

($t < 0.05s$) are similar to the segregated approach, the later results deviate due to the nature of the FCT scheme: it does not appropriately deal with vorticity. Similar to the previous case, the computational cost is somewhat lower than the segregated approach, but not as much as expected due to the values of the density at the cell faces.

Eulerian-Lagrangian method

For the Eulerian-Lagrangian method, we have compared the results to our earlier work in this field van Wachem et al. (2001), in which we employed a staggered segregated approach coupled to a Lagrangian particle phase. In the current simulation 31,000 particles ($d_p = 1.54mm$, $\rho_p = 1150kgm^{-3}$) are simulated in a fully 3 dimensional set-up, see Figure 6(a). The set-up is a fluidized bed van Wachem et al. (2001) with a uniform inlet of air, and additionally contains an air jet in the bottom region. Initially,

the particles are placed in a square region just above the jet, see Figure 6(b).

Figure 6(c) shows the location of the particles and

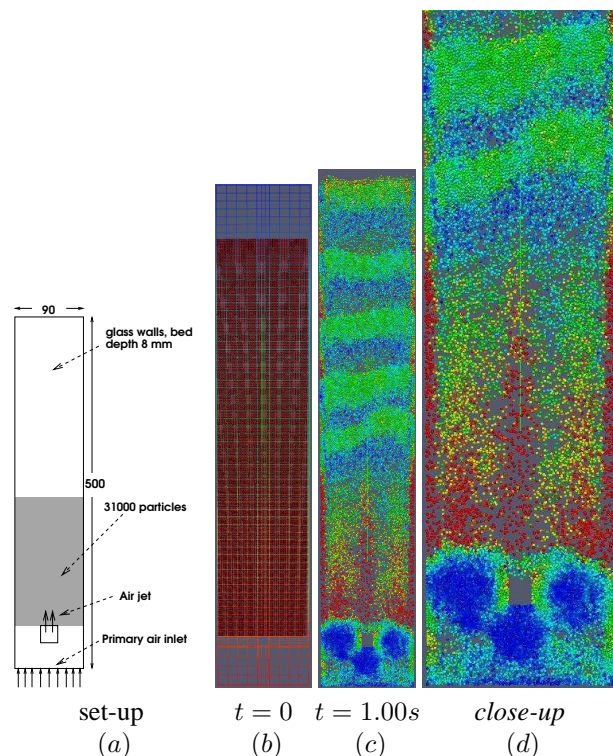


Figure 6: (a) The set-up employed in this work, from van Wachem et al. (2001) with additional injector, (b) the initial particle conditions including the gas-phase grid, (c) the particle locations and velocities (color) after 1.0 s, (d) a close-up of the bottom part of figure (c).

the velocity of the particles, denoted by their color, after 1.00 s of real time. Figure 6(d) shows a close-up of the bottom region of the fluidized bed. Although the results obtained in van Wachem et al. (2001) are only two-dimensional, the over-all behaviour matches well with what is seen in practice. Moreover, a relatively grid-independent solution is obtained, which is often a problem in Eulerian-Lagrangian simulations.

In this case, the fully coupled solver for the gas-phase performs much faster and more robust than the segregated approach described in van Wachem et al. (2001). The computational cost of solving the gas phase is almost three times less with the fully coupled approach. Moreover, the treatment of source terms as outlined earlier, makes this approach more robust as its segregated counterpart. Unfortunately, the computational cost for solving the gas phase is only a fraction of the computational cost for solving the paths of all the particles.

Conclusions

A fully coupled method has been proposed and employed for solving two types of multiphase flows, *i.e.* a volume of fluid (VOF) method, and a Eulerian-Lagrangian particle

method. Momentum weighted interpolation of the discretized momentum equations by finite volumes is used to determine analytical expressions for the cell face velocities. These are employed in the finite volume discretisation of the multiphase continuity equation in a collocated variable arrangement, which leads to a fully coupled matrix with the velocities and pressure as the unknown variables. A special approach is adopted for the momentum weighted interpolation to handle large source terms, volume fractions, densities, and gradients of these.

For the VOF method employed in this work, two cases are compared with a segregated solver. Although there is an increase in robustness, and a decrease in computational cost compared to the staggered segregated approach, the decrease is relatively small due to the magnitude of some of the discretised coefficients. In the Eulerian-Lagrangian approach, one case is shown and a large increase in robustness and a large decrease in computational cost compared to the staggered segregated approach is reported.

The global and implicit treatment of the pressure-velocity coupling and the special treatment of source terms and volume fraction and density gradients in the main reason for the increased robustness. Currently, the limitation of the fully coupled approach is a computationally efficient and robust preconditioner and linear solver.

Remark: For the sake of brevity, some elements (discretisation, algorithms, meshes, configurations) that the reader may find interesting have not been shown here, but are available upon request of the authors.

Acknowledgements

We would like to thank George Raithby and Gordon Stubble from the University of Waterloo in Canada for their fruitful discussions and clear notes on computational fluid dynamics.

We would like to thank the Swedish Research Council (VR), the Swedish Energy Agency (STEM), and Bo Rydins research foundation for financial support.

References

I. Ammara and C. Masson. Development of a fully coupled control-volume finite element method for the incompressible navier-stokes equations. *Int. J. Numer. Meth. Fluids*, 44:pp. 621–644, 2004.

R. Aris. *Vectors, Tensors, and the Basic Equations of Fluid Mechanics*. Dover, 1962.

Satish Balay, William D. Gropp, Lois Curfman McInnes, and Barry F. Smith. Efficient management of parallelism in object oriented numerical software libraries. In E. Arge, A. M. Bruaset, and H. P. Langtangen, editors, *Modern Software Tools in Scientific Computing*, pages 163–202. Birkhäuser Press, 1997.

Satish Balay, Kris Buschelman, Victor Eijkhout, William D. Gropp, Dinesh Kaushik, Matthew G. Knepley, Lois Curfman McInnes, Barry F. Smith, and Hong Zhang. PETSc users manual. Technical Report ANL-95/11 - Revision 2.1.5, Argonne National Laboratory, 2004.

Satish Balay, Kris Buschelman, William D. Gropp, Dinesh Kaushik, Matthew G. Knepley, Lois Curfman McInnes, Barry F. Smith, and Hong Zhang. PETSc Web page, 2006. <http://www.mcs.anl.gov/petsc>.

J.P. Boris and D.L. Book. Flux-corrected transport i: Shasta, a fluid transport algorithm that works. *J. Comput. Phys.*, 11: pp. 38–69, 1973.

J.U. Brackbill, D.B. Kothe, and C. Zemach. A continuum method for modeling surface tension. *J. Comp. Phys.*, 100: 335–354, 1992.

A.M. Bruaset. *A survey of preconditioned iterative methods*. Longman group, England, 1995.

S.-K. Choi, S.-O. Kim, C.-H. Lee, and H.-K. Choi. Use of the momentum interpolation method for flows with a large body force. *Numerical heat transfer, Part B.*, 43:267–287, 2003.

G.B. Deng, J. Piquet, P. Queutey, and M. Visonneau. Incompressible flow calculations with a consistent physical interpolation finite volume approach. *Computers Fluids*, 23:1029–1047, 1994.

G.B. Deng, J. Piquet, X. Vasseur, and M. Visonneau. A new fully coupled method for computing turbulent flows. *Computers and Fluids*, 30:pp. 445–472, 2001.

J.H. Ferziger and M. Peric. *Computational Methods for Fluid Dynamics*. Springer, 2002.

U. Ghia, KN Ghia, and CT Shin. High-re solutions for incompressible flow using the navier-stokes equations and a multi-grid method. *Journal of Computational Physics*, 48:387–411, 1982.

F.H. Harlow and J.E. Welch. Numerical calculation of time-dependent viscous incompressible flow of fluid with a free surface. *Physics of Fluids*, 8:pp. 2182–2189, 1965.

C.W. Hirt and B.D. Nicholls. Volume of fluid (VOF) method for the dynamics of free boundaries. *J. Comp. Phys.*, 39:201, 1981.

B.P.B. Hoomans, J.A.M. Kuipers, W.J. Briels, and W.P.M. van Swaaij. Discrete particle simulation of bubble and slug formation in a two-dimensional gas-fluidised bed: A hard-sphere approach. *Chem. Eng. Sci.*, 51(1):99–118, 1996.

R. Jackson. Locally averaged equations of motion for a mixture of identical spherical particles and a newtonian fluid. *Chem. Eng. Sci.*, 52:2457–2469, 1997.

A.J.C. Ladd and O.R. Walton. Granular flow: Numerical simulation of dry granular flows and calculation of hydrodynamic interactions in suspensions. Technical Report UCRL-101605, Lawrence Livermore National Laboratory, 1989.

A.W. Lees and S.F. Edwards. The computer study of transport processes under extreme conditions. *J. Phys. C*, 5:1921–1929, 1972.

S.V. Patankar. *Numerical Heat Transfer and Fluid Flow*. Hemisphere Publishing Corporation, 1980.

B. Perot. Conservation properties of unstructured staggered mesh schemes. *Journal of Computational Physics*, 159:58–89, 2000.

C.M. Rhie and W.L. Chow. Numerical study of the turbulent flow past an airfoil with trailing edge separation. *AIAA JI*, 21:1527–1532, 1983.

M. Rudman. Volume-tracking methods for interfacial flow calculations. *Int. J. Numer. Methods Fluids*, 24:671, 1997.

G.E. Schneider and M.J. Raw. Control volume finite-element method for heat transfer and fluid flow using collocated variables - 1. computational procedure. *Numerical Heat Transfer*, 11:363–390, 1987.

B.G.M. van Wachem and J.C. Schouten. Experimental validation of 3-d lagrangian VOF model: bubble shape and rise velocity. *AIChE J.*, 48:2744–2753, 2002.

B.G.M. van Wachem, J. van der Schaaf, J.C. Schouten, R. Krishna, and C.M. Van den Bleek. Experimental validation of lagrangian-eulerian simulation of fluidized beds. *Powder Technology*, 116:155–165, 2001.

S.P. Vanka. Block-implicit calculation of steady turbulent recirculating flows. *Int. J. Heat and Mass Transfer*, 28:pp. 2093–2103, 1985.

O.R. Walton. Numerical simulation of inclined chute flows of monodisperse, inelastic, frictional spheres. *Mechanics of Materials*, 16:239–247, 1993.

I. Wenneker, A. Segal, and P. Wesseling. Conservation properties of a new unstructured staggered scheme. *Computers and Fluids*, 32:pp. 139–147, 2003.

P. Wesseling. *Principles of Computational Fluid Dynamics*. Springer, Berlin, Germany, 2000.

P. Wesseling, A. Segal, C.G.M. Kassels, and H. Bijl. Computing flows on general two-dimensional nonsmooth staggered grids. *Journal of Engineering Mathematics*, 34:21–44, 1998.

S.T. Zalesak. Fully multi-dimensional flux corrected transport algorithms for fluid flow. *J. Comput. Phys.*, 31:pp. 335–362, 1979.

P.J. Zwart. *The integrated space-time finite volume method*. PhD thesis, University of Waterloo, Canada, 1999.